Title

Seasonal Dynamics and Interannual Variability in Mercury Concentrations and Loads through a Three-Reservoir Complex

Journal

Environmental Science and Technology, 54(15)

ISSN

0013-936X

Authors

Baldwin, Austin K
Poulin, Brett A
Naymik, Jesse
et al.

Publication Date

2020-08-04

DOI

10.1021/acs.est.9b07103

Peer reviewed

Environmental Science & Technology

pubs.acs.org/est

Article

Seasonal Dynamics and Interannual Variability in Mercury Concentrations and Loads through a Three-Reservoir Complex

Austin K. Baldwin,* Brett A. Poulin, Jesse Naymik, Charles Hoovestol, Gregory M. Clark, and David P. Krabbenhoft

Cite This: https://dx.doi.org/10.1021/acs.est.9b07103

Read Online

ACCESS | Metrics & More | Article Recommendations | Supporting Information

ABSTRACT: The Hells Canyon Complex (HCC) along the Snake River (Idaho−Oregon border, U.S.A.) encompasses three successive reservoirs that seasonally stratify, creating anoxic conditions in the hypolimnion that promote methylmercury (MeHg) production. This study quantified seasonal dynamics and interannual variability in mercury concentrations (inorganic divalent mercury (IHg) and MeHg) and loads at four reservoir inflow and outflow locations through the HCC (2014−2017). We observed (1) that the HCC is a net sink for both IHg and MeHg, (2) interannual variability in IHg and MeHg loads largely reflecting streamflow conditions, and (3) seasonal variability in particulate IHg loading at the inflow (greatest from February to April) and MeHg export from the outflow (greatest from September to December) of the HCC. Seasonal export of MeHg was evidenced by increases in monthly mean concentrations of unfiltered MeHg (approximately 2-fold) and the percentage of total mercury (THg) as MeHg (≥4-fold) coincident with reservoir destratification. Despite evidence of seasonal export of MeHg from the HCC, annual loads indicate a 42% decrease in unfiltered MeHg from HCC inflow to outflow. Results from this study improve the understanding of seasonal variability in mercury transport through and transformation within a reservoir complex.

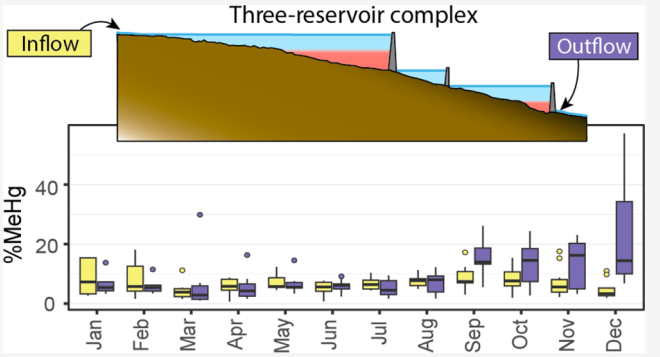

INTRODUCTION

Reservoirs are important freshwater aquatic environments for the conversion of inorganic divalent mercury (IHg) to neurotoxic methylmercury (MeHg).[1−3] The methylation of IHg is carried out by anaerobic bacteria (e.g., sulfate- or iron-reducing bacteria) and archaea under conditions of low dissolved oxygen and available labile organic matter.[4−7] Conditions conducive to IHg methylation are common in reservoirs, especially those which thermally stratify seasonally, with a layer of warm, oxygenated water near the surface and colder, anoxic or suboxic water at depth.[8,9] Consequently, mercury accumulates as MeHg in fish-tissue[10] to elevated concentrations in reservoirs compared to natural lakes,[3] often leading to fish consumption advisories and concerns for wildlife and human health.

Important knowledge gaps are whether seasonally stratified reservoirs act as a net source or net sink of MeHg to downstream waters, and the fate of MeHg formed at depth in a reservoir following reservoir destratification. Information on these research areas are needed to (1) identify the downstream environmental and human health impacts of reservoirs, (2) guide reservoir management, and (3) inform regulators tasked with developing total maximum daily loads (TMDLs) for reservoirs. Spatial and temporal patterns of MeHg production within a reservoir will be influenced by the inflow of IHg, labile carbon, availability of terminal electron acceptors, and the timing and duration of thermal and redox stratification, among other variables.[11,12] In contrast, the fate of hypolimnetic MeHg released from a reservoir will be controlled by the timing and duration of thermal destratification.[8,13] Previous studies have reported seasonally elevated MeHg concentrations at reservoir outflow versus inflow locations,[1,8,14,15] suggesting that MeHg produced within a reservoir can be exported downstream. MeHg accumulates in primary producers at significantly higher rates than IHg.[10] Reservoirs are effective environments for trophic transfer of MeHg to fish[16,17] compared to natural lakes,[3] in part due to elevated MeHg relative to total Hg (% MeHg). Despite these observations, few studies have quantified annual loads for IHg and MeHg to determine if a reservoir is a source or sink of MeHg to downstream aquatic

Received: November 22, 2019
Revised: April 13, 2020
Accepted: June 30, 2020

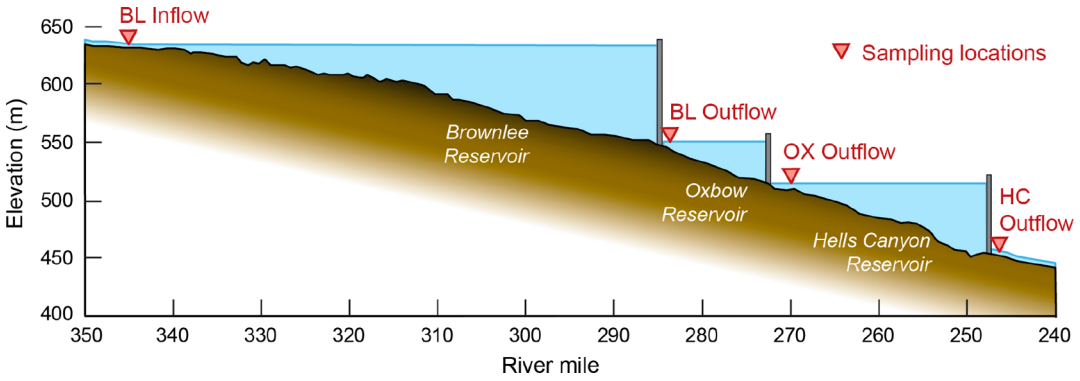

Figure 1. Sampling locations shown on a longitudinal cross-section view of the three reservoirs of the Hells Canyon Complex (HCC), Idaho–Oregon border, U.S.A. BL, Brownlee; OX, Oxbow; and HC, Hells Canyon.

environments,[18,19] or have assessed mercury behavior across seasons or between years of contrasting hydrologic conditions.

This investigation presents an in-depth assessment of concentrations and annual loads of different mercury species through a reservoir complex impaired for mercury.[20] We report inflow and outflow mercury concentrations at high temporal resolution under contrasting hydrologic conditions (i.e., high vs low streamflow years) through the three reservoirs of the Hells Canyon Complex (HCC). In addition, we report calculated inflow and outflow loads for filter-passing and particulate IHg and MeHg fractions. Results from this study improve the understanding of seasonal variability in mercury transport through and transformation within a reservoir complex. Findings from this effort, in conjunction with complementary ongoing research on the biogeochemical factors affecting mercury transformations in the reservoir complex, will inform conceptual and quantitative models designed to predict mercury behavior in the HCC under various reservoir management scenarios and hydrologic conditions.

METHODS

Study Area. The HCC consists of three hydroelectric reservoirs, built between 1958 and 1967, spanning approximately 90 river miles (145 km) of the Snake River along the Idaho–Oregon border (U.S.A.).[21] Upstream to downstream, the reservoirs are Brownlee, Oxbow, and Hells Canyon (Figure 1). Brownlee Reservoir is the largest of the three reservoirs in surface area (61 km^2), length (93 km), and volume (1752 million m^3), is the deepest (maximum depth of 91 m), and has the longest retention time (34 days; Supporting Information, SI, Table S1). Oxbow Reservoir is the smallest of the three reservoirs by all the same measures. Water levels commonly fluctuate by 15 m (up to 30 m maximum) in Brownlee Reservoir, mostly associated with flood control.[21] Water-level fluctuations in Oxbow and Hells Canyon Reservoirs are limited to approximately 1.5 m. A description of the study basin is provided in the SI.

The Snake River transports nutrients, organic matter, sediment, and mercury and other contaminants from the basin into the HCC.[21] In the early summer, the warming of both incoming water and the reservoir surfaces causes Brownlee and Hells Canyon Reservoirs to thermally stratify;[21,22] Oxbow Reservoir does not thermally stratify because of the shallower depth. Concurrent with thermal stratification of Brownlee and Hells Canyon Reservoirs is the decomposition of allochthonous and autochthonous organic matter, resulting in dissolved oxygen utilization at depth in the reservoirs. By July or August, Brownlee and Hells Canyon Reservoirs are typically completely stratified and anoxic throughout the hypolimnion and in parts of the metalimnion. In Brownlee Reservoir, the anoxia may extend from the dam (River Mile 285) up to River Mile 323, approximately 38 miles. Seasonal water-column sampling of these reservoirs has shown that MeHg concentrations in the metalimnion and hypolimnion are greater during periods of stratification.[20] The breakdown of thermal stratification in Brownlee Reservoir begins as early as August and is typically complete by late December.[22] The fate of the MeHg accumulated within the stratified reservoirs is unclear during and after destratification.

Fish-tissue data from the complex show that hypolimnetic MeHg is entering the food web: 31% of smallmouth bass collected in 2013 within the HCC and up to 60 miles downstream exceeded the State of Idaho human health fish-tissue criterion for mercury (0.3 mg/kilogram wet weight),[20] compared to 0% of smallmouth bass collected ∼177 km upstream of the HCC in the same year.[23] There is interest in understanding bioaccumulation within the reservoirs and the potential downstream export of MeHg to the lower Snake and Columbia Rivers. These rivers support populations of economically and culturally important fish species such as bull trout (*Salvelinus confluentus*) and fall Chinook salmon (*Oncorhynchus tshawytscha*), both listed under the Endangered Species Act, and white sturgeon (*Acipenser transmontanus*).

Sample Collection and Analysis. Water samples were collected at four locations representing the inflow and outflow of the three HCC reservoirs (Figure 1). From upstream to downstream, these locations were Brownlee Reservoir Inflow (Brownlee Inflow), Brownlee Reservoir Outflow (Brownlee Outflow), Oxbow Reservoir Outflow (Oxbow Outflow), and Hells Canyon Reservoir Outflow (Hells Canyon Outflow). Mean daily streamflow data for Brownlee Inflow and Hells Canyon Outflow were from USGS streamgage stations 13269000 and 13290450, respectively.[24] Mean daily streamflow data for Brownlee Outflow and Oxbow Outflow were from Idaho Power Company. Samples were collected biweekly from October 2013 through December 2017 (n = 100–103 per location), with breaks in January to February 2015 and January 2016 when sampling was not possible because of harsh weather conditions.

Samples were collected and processed using ultraclean trace-metal protocols.[25] Collection methods included depth-integrated and grab sampling, depending on location (details

https://dx.doi.org/10.1021/acs.est.9b07103
Environ. Sci. Technol. XXXX, XXX, XXX–XXX

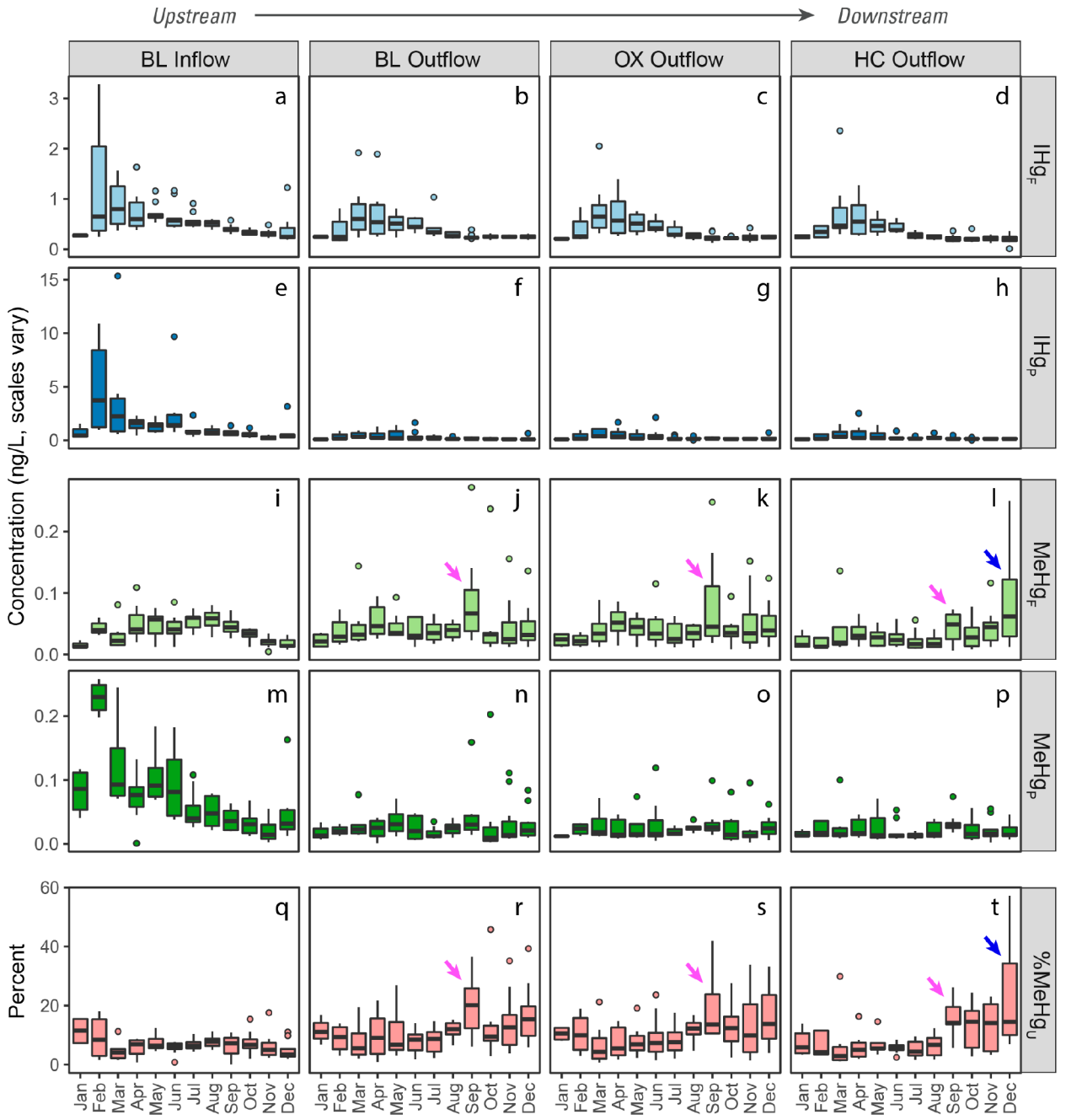

Figure 2. Concentrations of filter-passing divalent inorganic mercury (IHg_F), particulate divalent inorganic mercury (IHg_P), filter-passing methylmercury ($MeHg_F$), and particulate methylmercury ($MeHg_P$), and unfiltered MeHg as a percentage of unfiltered total mercury ($\%MeHg_U$) at the Hells Canyon Complex reservoir inflow and outflow locations, October of 2013 through December of 2017. Number of samples per month = 3−12. Box plots present median and quartile ranges of constituent concentrations or fractions (n = 3−12), whiskers extend 1.5× the interquartile range, and outliers are shown as points. Pink arrows identify the September increase in $MeHg_F$ and $\%MeHg_U$ at outflow locations, and blue arrows identify the December increase in $MeHg_F$ and $\%MeHg_U$ at Hells Canyon Outflow. [BL, Brownlee; OX, Oxbow; HC, Hells Canyon].

in the SI). Samples were stored in the dark on ice, and within 24 h of collection were passed through a quartz fiber filter (0.7 μm pore size, precombusted 550 °C) to isolate the particulate and filter-passing fractions for THg and MeHg quantification.[26] Particulate fractions were frozen at −20 °C on the filters and stored in the dark. Filter-passing fractions were stored in Teflon bottles and acidified to 1% volume-to-volume with ultraclean hydrochloric acid.

Samples collected October 2013 through June 2014 (n = 94) were analyzed for filter-passing and unfiltered THg and MeHg by Battelle Marine Sciences Laboratory (Battelle) in Sequim, Washington. THg was analyzed using cold vapor atomic fluorescence spectrometry (CVAFS) according to U.S. EPA Method 1631, Revision E.[27] MeHg was analyzed according to U.S. EPA Method 1630.[28] Particulate THg (THg_P) and MeHg ($MeHg_P$) were calculated by subtracting the filter-passing concentrations from the unfiltered concentrations.

Samples collected from June 2014 through December 2017 (n = 306) were analyzed for filter-passing and particulate THg (THg_F, THg_P) and MeHg ($MeHg_P$, $MeHg_F$) by the USGS Mercury Research Laboratory (MRL) in Middleton, Wiscon-

https://dx.doi.org/10.1021/acs.est.9b07103
Environ. Sci. Technol. XXXX, XXX, XXX−XXX

sin. THg was analyzed using USEPA Method 1631, Revision E,[27] with modifications by the MRL.[26] MeHg was analyzed according to U.S. EPA Method 1630,[28] modified as described in USGS Open-File Report 01−445[29] to use Hg isotope dilution and inductively coupled plasma mass spectrometry detection for improved low-level detection. Unfiltered THg (THg_U) and MeHg ($MeHg_U$) were computed by adding the filtered and particulate fractions. Inorganic Hg (IHg) concentrations (IHg_P, IHg_F) were calculated by subtracting MeHg from THg for particulate and filter-passing fractions, respectively. The quality control/quality assurance (QAQC) section in the SI details a comparison of duplicate samples analyzed by both Battelle and the MRL (Figure S1) and results of field blanks and field replicates.

Vertical profiles of water temperature and dissolved oxygen were measured in Brownlee Reservoir at River Mile 286, one mile upstream of Brownlee Dam, to provide information on the stratification state of Brownlee Reservoir. These data were collected up to three times per month through the spring, summer, and fall months of the study period. In winter months profiles were collected infrequently because of harsh weather conditions and icy boat ramps.

Data Analysis. Historical streamflow statistics for Brownlee Inflow were computed using the period 1968−2017, as most of the upstream reservoirs affecting streamflow were completed by 1968. R software packages *dplyr* and *stats* were used to compute summary statistics and streamflow percentiles.[30,31]

Analytical results less than the daily detection limit (DDL) for mercury were substituted at one-half the DDL for all analyses except load estimation (described in the SI). An assessment of whether the use of one-half DDL substitution biased the results is described in the SI. Inorganic divalent mercury (IHg) concentrations were computed by subtracting MeHg from THg concentrations, using one-half the DDL for values below the DDL.

Interannual variability in mercury concentrations was assessed using the Kruskal−Wallis multiple comparisons test ($p < 0.05$; using the kruskalmc function in the R package *pgirmess*[32]). Other comparisons, such as those across sites or across months, are observational. The percentage of THg_U as $MeHg_U$ ($\%MeHg_U$) was used as an indicator of in-reservoir processes influencing MeHg abundance (i.e., methylation and demethylation). An increase in $\%MeHg_U$ from inflow to outflow was interpreted to indicate net methylation within the reservoir, and a decrease indicated net loss terms (e.g., demethylation,[11,33] sedimentation).

Daily and annual loads were estimated for each site and constituent using *rloadest*,[34] an R software package based on the FORTRAN program LOADEST[35] (details provided in the SI). For each constituent, a mean daily load was computed for each site over the four-year period January 2014 to December 2017 using the *rloadest*-estimated daily loads. Daily load estimates for 2013, which were limited to October to December, were excluded from the mean daily load calculation to avoid biasing results toward those months. Net gains or losses in mean daily loads through each reservoir were computed by subtracting the outflow from the inflow. Brownlee Outflow is considered the inflow to Oxbow Reservoir, and Oxbow Outflow is considered the inflow to Hells Canyon Reservoir. Load estimation model diagnostics are provided in SI Table S2. Model coefficients of determination (R^2) ranged from 34.4 to 94.2, with a median of 81.4 (p-values on all models were <0.0001). The load bias statistic (Bp) and the partial load ratio (PLR) both indicated minimal over- or under-estimation in the majority of models: the Bp was less than ±10% for 35/36 models, and the highest Bp was 15.9%.

All data collected as part of this study are publicly available from the USGS National Water Information System.[24]

RESULTS

Streamflow. The streamflow of the Snake River at Brownlee Inflow varied considerably during the study period. Annual mean daily streamflow ranged from 289 m^3/s in 2013 to 717 m^3/s in 2017. For comparison, the historical annual mean daily streamflow was 492 m^3/s (1968−2016; minimum 251 m^3/s, maximum 956 m^3/s). The greatest interannual variability occurred during the March to June period, when 2017 streamflows were historically high, and 2015 streamflows were historically low (SI Figure S3). Mean daily streamflows in March through May of 2017 were ≥90th percentiles of historical flows, as compared to the ≤14th percentiles in 2015. In the autumn and winter months, streamflows were generally low in 2013−2016 and moderate in 2017 as compared to historical records.

Seasonality in Mercury Concentrations. Over the study period (October 2013 to December 2017) concentrations of IHg_U, IHg_P, and IHg_F at Brownlee Inflow averaged 1.89 ng/L, 1.35 ng/L, and 0.55 ng/L, respectively, but varied considerably by season. Monthly median concentrations dramatically increased from January to February, were greatest in February (IHg_U, 4.36 ng/L; IHg_P, 3.72 ng/L) and March (IHg_F, 0.80 ng/L), and gradually decreased through the summer months to the lowest levels in November (IHg_U, 0.60 ng/L; IHg_P, 0.26 ng/L) and December (IHg_F, 0.24 ng/L) (Figure 2a,e; SI Table S5). The same seasonal patterns of IHg_U,IHg_P, and IHg_F observed at Brownlee Inflow were observed at the three reservoir outflow locations, but at lower concentrations (Figure 2). Monthly median IHg_U, IHg_P, and IHg_F concentrations at reservoir outflow locations were highest in March and April (IHg_U, 0.90−0.96 ng/L; IHg_P, 0.22−0.37 ng/L; IHg_F, 0.47−0.65 ng/L) and lowest in September to January (IHg_U, 0.31−0.41 ng/L; IHg_P, 0.09−0.17 ng/L; IHg_F, 0.19−0.25 ng/L) (Figure 2a−h; SI Table S5). The seasonal behavior of THg across the HCC were comparable to that of IHg (THg results provided in SI Table S5).

Concentrations of $MeHg_U$, $MeHg_P$, and $MeHg_F$ at Brownlee Inflow averaged 0.106 ng/L, 0.068 ng/L, and 0.038 ng/L, respectively, over the study period. $MeHg_P$ concentrations at Brownlee Inflow followed the seasonal pattern observed in IHg concentrations, with monthly medians being highest in February (0.230 ng/L) and lowest in November (0.014 ng/L; Figure 2m; SI Table S5), likely driven by differences in suspended particle concentration. The seasonal pattern in $MeHg_P$ concentrations at reservoir outflow locations was distinctly different from that at Brownlee Inflow. Specifically, $MeHg_P$ concentrations exhibited no seasonal pattern and were not statistically different across most months (Figure 2n−p; SI Table S5). $MeHg_F$ concentrations at Brownlee Inflow exhibited a seasonal pattern distinct from that observed for other mercury fractions, with concentrations gradually increasing through spring and reaching a maximum in July (median 0.060 ng/L), then gradually decreasing through autumn to reach a minimum in January (median 0.013 ng/L) (Figure 2i; SI Table S5). However, this seasonal pattern was

https://dx.doi.org/10.1021/acs.est.9b07103
Environ. Sci. Technol. XXXX, XXX, XXX−XXX

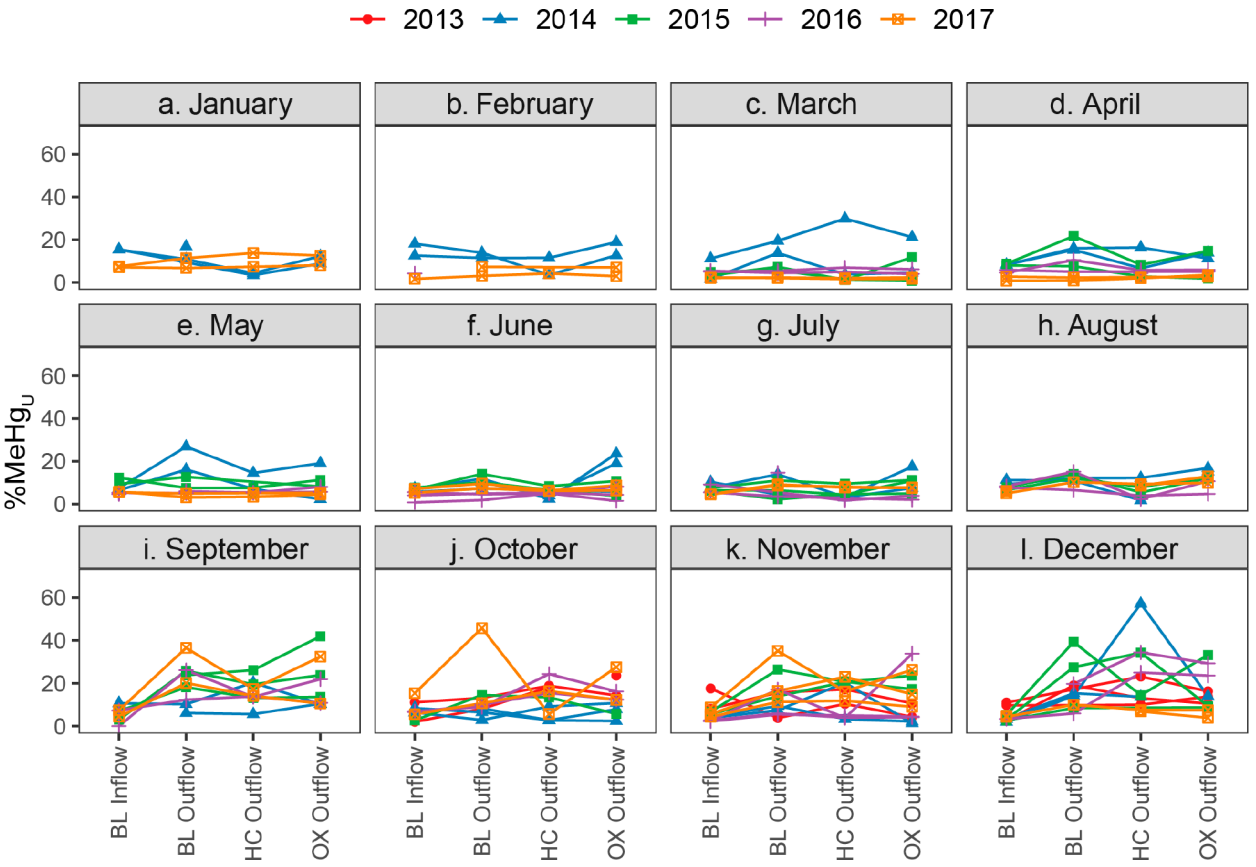

Figure 3. Percentage of unfiltered total mercury as methylmercury ($\%MeHg_U$) by month at Hells Canyon Complex inflow and outflow locations, 2013−2017. Each line represents a sampling event. Sampling locations are ordered upstream to downstream, left to right.

not observed at Brownlee Outflow. Rather, median $MeHg_F$ concentrations at Brownlee Outflow exhibited a marked increase between August and September (0.040 to 0.067 ng/L), followed by a decrease of similar magnitude from September to October (0.067 to 0.032 ng/L) (Figure 2j, pink arrow; SI Table S5). The September median $MeHg_F$ concentration at Brownlee Outflow was 52% greater than that at Brownlee Inflow. The marked increase in $MeHg_F$ concentrations between August and September at Brownlee Outflow was also observed at Oxbow Outflow and Hells Canyon Outflow, albeit to a lesser degree (Figure 2k,l, pink arrows; SI Table S5). At Hells Canyon Outflow, we observed elevated $MeHg_F$ concentrations in December (median of 0.062 ng/L; Figure 2l, blue arrows) that exceeded Oxbow Outflow by 59%, Brownlee Outflow by 94%, and Brownlee Inflow by 343%.

IHg and MeHg were predominantly present in the particulate phase at Brownlee Inflow and in the filter-passing phase at the three reservoir outflow locations (average of 61.8% and 58.3%, respectively, n = 103; SI Figure S4; SI Table S7). At Brownlee Inflow seasonal variation was observed in the percentage of IHg and MeHg in the particulate versus filter-passing phases, with the percent particulate exhibiting maxima in January (MeHg, mean 84.4%, n = 4) or February (IHg, 80.0%; n = 4), a decreasing trend through spring and summer, and minima in November (42.0% and 43.1% for IHg and MeHg, respectively; n = 12). At the three reservoir outflow locations, IHg and MeHg were primarily in the filter-passing phase (% particulate mean values of 35.1−41.1% and 36.3−39.9%, respectively, across all samples, n = 100−102) and exhibited less seasonal variability compared to Brownlee Inflow.

The percentage of THg_U as $MeHg_U$ ($\%MeHg_U$) varied by site and season, averaging 6.5% at Brownlee Inflow (n = 103), 12.0% at Brownlee Outflow (n = 102), 11.4% at Oxbow Outflow (n = 102), and 10.2% at Hells Canyon Outflow (n = 100). The greatest variability in $\%MeHg_U$ was observed in Brownlee Reservoir (i.e., between Brownlee Inflow and Brownlee Outflow), where median $\%MeHg_U$ exhibited modest increases (<4.2 percentage points) between January and August (Figure 3a-3h) but dramatic increases (7.6−12.9 percentage points) in September, November, and December (Figure 3i,k,l; SI Table S9). The greatest $\%MeHg_U$ increases from the inflow to outflow of Brownlee Reservoir typically were observed in September, when median $\%MeHg_U$ increased from 7.2% to 20.1% (Figure 3i). A similar increase in $\%MeHg_U$ from Brownlee Inflow to Outflow was observed in December, when median$\%MeHg_U$ increased from 3.4% to 15.3% (Figure 3l). Changes in $\%MeHg_U$ through Oxbow and Hells Canyon Reservoirs were relatively minor: between January and September, $\%MeHg_U$ typically decreased from inflow to outflow by up to 6 percentage points; and, between October and December, $\%MeHg_U$ was typically unchanged or modestly increased from inflow to outflow (Figure 3; SI Tables S8 and S9).

Interannual Variability in Mercury Concentrations. The interannual variability in mercury concentrations at each site was assessed using the Kruskal−Wallis multiple comparisons test (p-value <0.05). The statistical significance of each year-to-year comparison is shown in SI Figure S4 and Figure 4.

https://dx.doi.org/10.1021/acs.est.9b07103
Environ. Sci. Technol. XXXX, XXX, XXX−XXX

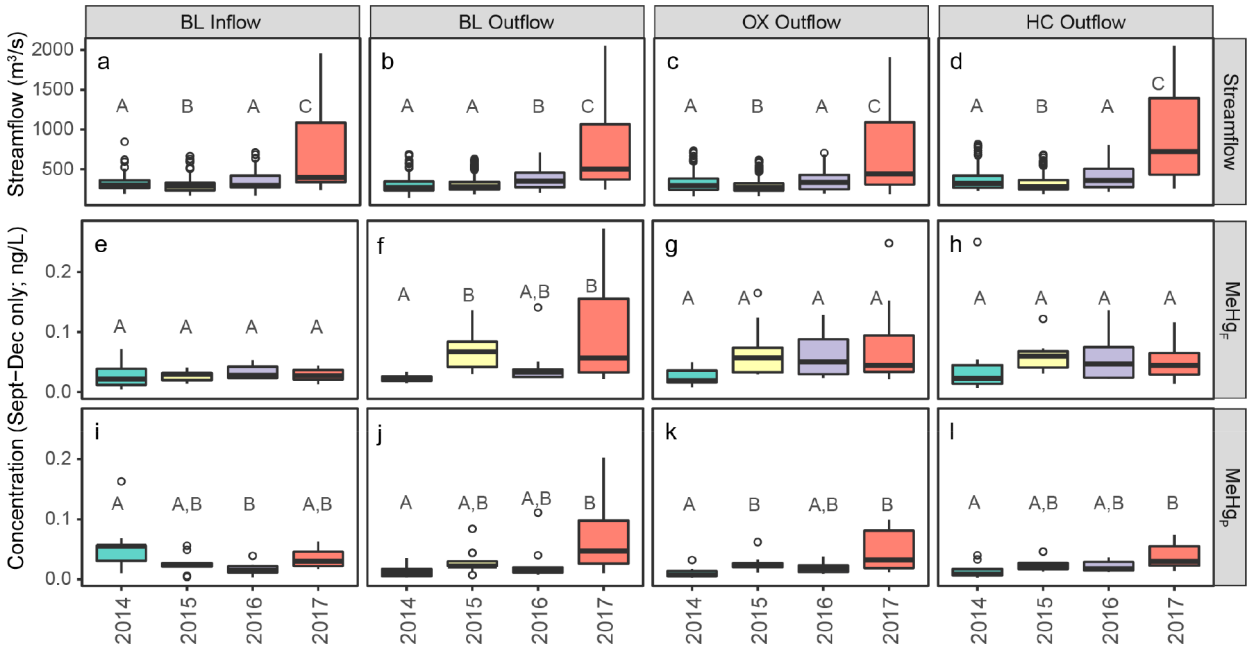

Figure 4. Streamflow and concentrations of filter-passing ($MeHg_F$) and particulate methylmercury ($MeHg_P$) at Hells Canyon Complex inflow and outflow locations, 2014–2017. Streamflows are daily means for the entire year and are in cubic meters per second (m^3/s). Concentrations are discrete samples between September and December only (n = 8–9 per site per year) and are in nanograms per liter (ng/L). Boxplots present median and quartile ranges, whiskers extend 1.5× the interquartile range, and outliers are shown as points. Boxplot labels ("A", "B", "C") indicate which years are statistically similar (those sharing a common letter) and statistically different (those not sharing a common letter) using the Kruskal–Wallis multiple comparisons test (p-values <0.05). [BL, Brownlee; OX, Oxbow; HC, Hells Canyon].

At all sites, IHg_U concentrations primarily reflected differences in streamflow. Higher streamflows in 2017 (March to June, SI Figure S3) corresponded with higher concentrations of IHg_U, and low streamflows in 2015 corresponded with low concentrations of IHg_U (SI Figure S5, SI Table S6). The effect of streamflow on $MeHg_U$ concentrations was less clear. $MeHg_U$ at Brownlee Inflow was highest in a moderate streamflow year (2014) as compared to other study years with both historical high (e.g., 2017) and historical low (2015) flows. $MeHg_U$ concentrations at the three outflow locations were modestly higher in 2017 as compared to 2014–2016 (SI Figure S5).

To understand the influence of streamflow on MeHg export from the HCC, we evaluated $MeHg_F$ and $MeHg_P$ concentrations during the time period associated with reservoir destratification (September to December; SI Figure S6).[22] At Brownlee Inflow, there were no significant differences in $MeHg_F$ concentrations from September to December between 2014 and 2017, despite significant year-to-year differences in streamflow (Figure 4a,e and SI Figure S3). From September to December, $MeHg_F$ concentrations at the three reservoir outflow locations were more variable than at Brownlee Inflow, but no trend between $MeHg_F$ concentration and streamflow was observed. For example, $MeHg_F$ concentrations at Brownlee Outflow were elevated under both low- (2015) and high-flow years (2017; Figure 4b,f), suggesting that the streamflow conditions were not the primary controlling factor on $MeHg_F$ export from the reservoir complex. $MeHg_P$ concentrations in September to December at Brownlee Inflow were highest in 2014, a moderate streamflow year (Figure 4i). However, $MeHg_P$ concentrations at the three reservoir outflow locations were highest in 2017 (Figure 4j–l), the high flow year, suggesting a positive relation with streamflow.

Mean Daily Mercury Loads. Mean daily loads were estimated for the four-year period January 2014 to December 2017. The mean daily load of IHg_P was 70.5 g/day at Brownlee Inflow and 18.4 g/day at Brownlee Outflow, which represents a net loss of 52.2 g/day through Brownlee Reservoir (Figure 5; SI Tables S10 and S11). Downstream of Brownlee Outflow, the mean daily load of IHg_P incrementally increased, to 19.6 g/day at Oxbow Outflow and 25.0 g/day at Hells Canyon Outflow. The observed IHg_P load increases are attributed to IHg_P contributions from side tributaries or nonpoint overland flow and/or sediment resuspension within reservoirs. Through the entire HCC, the mean daily load of IHg_P decreased by 45.6 g/day. The mean daily load of IHg_F was 28.2 g/day at Brownlee Inflow and 21.3 g/day at Brownlee Outflow, resulting in a net loss of 6.91 g/day through Brownlee Reservoir. The mean daily load of IHg_F remained constant at Oxbow Outflow and Hells Canyon Outflow. Through the entire HCC, the mean daily load of IHg_F decreased 7.32 g/day.

The mean daily load of $MeHg_P$ decreased from Brownlee Inflow (2.91 g/day) to Brownlee Outflow (1.06 g/day), resulting in a net loss of 1.85 g/day. Downstream of Brownlee Outflow, the mean daily load of $MeHg_P$ decreased slightly at Oxbow Outflow (0.95 g/day) and remained constant at Hells Canyon Outflow (0.96 g/day). Through the entire HCC, the mean daily load of $MeHg_P$ decreased 1.95 g/day. A modest increase in the mean daily load of $MeHg_F$ was observed from Brownlee Inflow (1.52 g/day) to Brownlee Outflow (1.75 g/day), followed by small, incremental decreases at Oxbow Outflow (1.71 g/day) and Hells Canyon Outflow (1.63 g/day). Through the entire HCC, the mean daily load of $MeHg_F$ increased by 0.11 g/day.

Interannual Variability in Mean Daily Mercury Loads. Constituent loads are partially dependent on streamflow, and therefore mercury loads varied considerably between the years

https://dx.doi.org/10.1021/acs.est.9b07103
Environ. Sci. Technol. XXXX, XXX, XXX–XXX

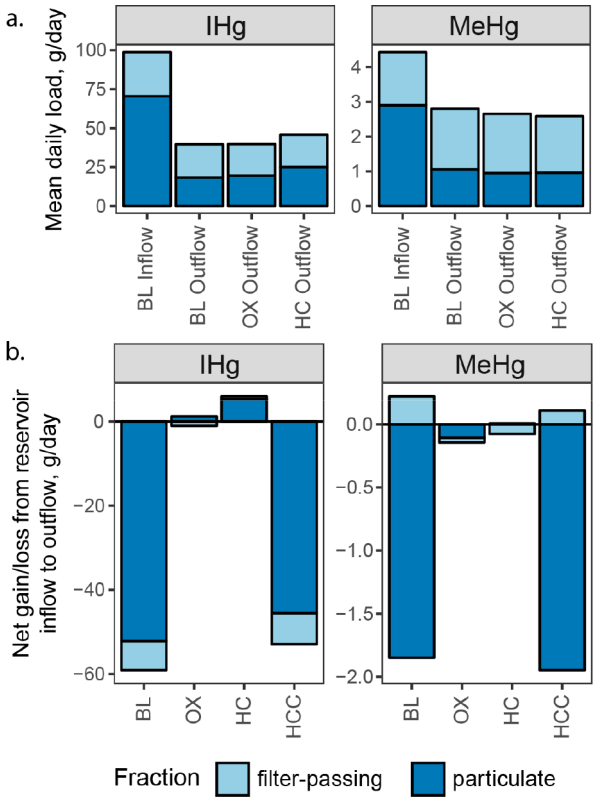

Figure 5. (a) Estimated mean daily loads of particulate and filter-passing divalent inorganic mercury (IHg) and methylmercury (MeHg) at Hells Canyon Complex (HCC) inflow and outflow locations, 2014−2017, and (b) the net gain (+) or loss (−) of mercury loads from reservoir inflow to outflow and the entire Hells Canyon Complex. [BL, Brownlee; OX, Oxbow; HC, Hells Canyon; and HCC, Hells Canyon Complex].

of this study. The historically high and low streamflows observed in 2017 and 2015 (annual means of 717 m^3/s and 292 m^3/s, respectively), likely approximate upper and lower bounds for mercury loads in the HCC. Annual mean daily loads of IHg_U at Brownlee Inflow ranged by greater than 6-fold from 36.1 g/day (2015) to 247 g/day (2017) (SI Figure S7; SI Table S12). IHg_U loads were lower at the three outflow locations, ranging from 13.4 to 14.3 g/day in 2015 to 106−146 g/day in 2017. Annual mean daily loads of $MeHg_U$ at Brownlee Inflow ranged from 2.71 g/day in 2015 to 8.14 g/day in 2017, a 3-fold difference. $MeHg_U$ loads were lower at the three outflow locations, ranging from 1.58 to 1.93 g/day in 2015 to 4.83−6.03 g/day in 2017. Annual mean daily loads of the filter-passing and particulate fractions are provided in SI Table S12.

DISCUSSION

This study described the occurrence and transport of mercury through the three reservoirs of the HCC and provides an assessment of the fate of MeHg accumulated in the water column following seasonal destratification. We report that (1) on an annual basis, the HCC is a sink for both IHg and MeHg, primarily due to retention of particulate material in Brownlee Reservoir (Figure 5); (2) there was a distinct increase in IHg_P loading into the HCC between February and April and in $MeHg_F$ export from HCC between September and December (Figure 2, 4); and (3) hydrologic conditions influence interannual variability in mercury loads to and from the HCC and potentially $MeHg_F$ releases between September and December (Figure 4 and SI Figure S7). We interpret the seasonal increase in $MeHg_F$ export from primarily Brownlee Reservoir to be a result of reservoir destratification (SI Figure S6).[22]

The concentrations of THg_U entering the HCC at Brownlee Inflow (median 1.34 ng/L) were moderate as compared to other streams in the U.S.A. (median 2.09 ng/L, n = 336),[36] despite mining-related mercury contamination in upstream sub-basins of the Snake River (e.g., the Owyhee Mountains[37]). The behavior of IHg_P and IHg_F upgradient and within the HCC (e.g., transport and aqueous-particulate partitioning) are likely controlled by interactions with POC and DOC, respectively.[38] $MeHg_U$ concentrations entering the HCC (median 0.09 ng/L at Brownlee Inflow) were comparable to those in other streams in the U.S.A. (median 0.11 ng/L, n = 337).[36] Similarly, MeHg concentrations at the Hells Canyon Outflow were moderate compared to other rivers even in the months with the highest MeHg concentrations (September and December). However, $\%MeHg_U$ in the HCC was elevated compared to streams across the conterminous USA ($MeHg_U$ nationwide median of 4.6%, n = 328[36]), especially at the three reservoir outflow locations. The median$\%MeHg_U$ at Brownlee Inflow, Brownlee Outflow, Oxbow Outflow, and Hells Canyon Outflow for the period of study was 6.3%, 10.3%, 10.5%, and 7.0%, respectively. Monthly median $\%MeHg_U$ levels at reservoir outflow locations were as high as 20.1%, and the maximum of discrete samples was 57.2% (Figure 2r−t; SI Table S8), which likely explains the observed increased in fish mercury levels in the reservoir complex.[20] We interpret the increase in $\%MeHg_U$ (Figure 2q−t) and $MeHg_F$ concentration (Figure 2i−l) from inflow to outflow to reflect the seasonal export of MeHg produced within the HCC. Similar observations have been made in Cottage Grove Reservoir (Oregon), where the %MeHg was shown to correlate with higher methylation rates within the reservoir.[11]

We propose that the observed seasonal variation in MeHg in the HCC is primarily driven by the seasonal stratification and destratification of Brownlee Reservoir (SI Figure S6). Brownlee Reservoir has the largest capacity of the three reservoirs and the largest volume of anoxic water (SI Table S1). Water column temperature and dissolved oxygen profiles of Brownlee Reservoir show onset of vertical stratification around late March and continuing through August,[22] providing a long period for potential MeHg production.[20] Around September, cooler water from the Snake River flows into Brownlee Reservoir and beneath the warm epilimnion, displacing the anoxic water in the upgradient portion of the reservoir and eroding the metalimnion.[22] In the fall (November or December), cold Snake River inflow water erodes the anoxic hypolimnion, resulting in complete destratification of Brownlee Reservoir (SI Figure S6).[22] We attribute periods of destratification of Brownlee Reservoir (September through December) to the coincident increases in $MeHg_F$ concentrations and $\%MeHg_U$ observed at Brownlee Outflow (Figure 2i,m,q). These findings support that a substantial portion of MeHg exported from the HCC in September through December is produced at depth in Brownlee Reservoir and subsequently transported through Oxbow and Hells Canyon Reservoirs downstream to the Snake River. It is unlikely that MeHg desorption from particles contributed to the observed increase in $MeHg_F$ in the water column based on previous studies of MeHg partitioning.[39,40]

https://dx.doi.org/10.1021/acs.est.9b07103
Environ. Sci. Technol. XXXX, XXX, XXX−XXX

We tentatively ascribe elevated concentrations of MeHg at outflow locations in September to partial destratification, and in December to complete destratification of both Brownlee and, to a lesser extent, Hells Canyon Reservoirs. On the basis of these interpretations, we posit that observed differences in the timing of MeHg export from the HCC across years of this study reflect temporal differences in the onset and conclusion of destratification in Brownlee Reservoir (Figures 3 and 4). Further, the magnitude of MeHg export from the HCC will likely depend on a multitude of biogeochemical factors controlling hypolimnetic MeHg accumulation,[11,12] including IHg availability (e.g., effects of DOC), the availability of carbon and terminal electron acceptors, physical conditions that influence microbial rates (e.g., hypolimnion temperature), and the duration of stratification. Ultimately, biogeochemical factors controlling MeHg accumulation and limnologic factors controlling reservoir stratification and destratification will govern interannual variability in MeHg export from the HCC. The fate of MeHg exported from the HCC to the Snake River is unknown at this time.

Despite evidence for seasonal MeHg production and export, the HCC on an annual basis acted as a net sink for MeHg. On average, only 58% of the $MeHg_U$ load entering the HCC at Brownlee Inflow exited the HCC at the Hells Canyon Outflow (Figure 5). Most of the net retention of $MeHg_U$ within the HCC was attributable to a decrease in the load of $MeHg_P$ in Brownlee Reservoir (−1.85 g/day). $MeHg_F$ increased (0.11 g/day) through the HCC. The net retention of MeHg through the HCC likely results from a combination of in-reservoir processes, most notably sedimentation as evidenced by reductions in $MeHg_P$ loads from Brownlee Inflow to Brownlee Outflow (SI Tables S5 and S10). However, the net retention of MeHg in Brownlee Reservoir may also reflect biotic uptake and degradation from biotic demethylation[41] and photodemethylation.[42] Streamflow in the Snake River was an important factor in the interannual variability in Hg loads to and from the HCC. IHg_U and $MeHg_U$ loads throughout the HCC were several times greater in high streamflow years as compared to low streamflow years.

The influence of the HCC on mercury accumulation in downstream fish and other biota is not clear. Mercury concentrations in water are not always a good predictor of biological uptake,[43,44] in part due to mercury levels in fish reflecting previous exposure and the physical movement of fish.[12] Further, export of mercury in filter-passing and particulate fractions does not account for mercury export by fish and plant material, the relative importance of which are unknown at this time. Downstream environmental impacts of the HCC will depend on the temporal behavior in mercury export (concentration, %MeHg) of abiotic (water, particles) and biotic pools (zooplankton, fish).[13,45,46]

The results presented here provide an in-depth understanding of mercury concentrations and loads through the HCC. Annually, the HCC acts as a net sink for both THg and MeHg, despite seasonal export of $MeHg_F$ coincident with reservoir destratification. Complementary ongoing research efforts aim to identify the biogeochemical factors responsible for mercury transport, aqueous-particulate partitioning, methylation, and biotic uptake within the reservoirs. Together, results will inform both conceptual and quantitative models designed to predict mercury behavior in the HCC under various reservoir management scenarios and hydrologic conditions, and may provide insight into the processes influencing mercury behavior in other reservoirs in the arid western U.S.A.

■ ASSOCIATED CONTENT

Supporting Information

The Supporting Information is available free of charge at https://pubs.acs.org/doi/10.1021/acs.est.9b07103.

Site characteristics, reservoir water temperature and dissolved oxygen profiles, hydrographs of daily mean streamflow, load model diagnostics, blank and replicate sample results, and result summaries (PDF)

Table S1, Physical characteristics of Brownlee, Oxbow, and Hells Canyon Reservoirs; Table S2, model diagnostics for estimation of divalent inorganic mercury, methylmercury, and total mercury loads; Table S3, comparison of results from field blanks versus regular samples; Table S4, summary of results on field replicate samples; Table S5, mjonthly concentration summaries for water samples; Table S6, annual mercury concentration summaries; Table S7, percentage of total mercury, methylmercury, and divalent inorganic mercury in the particulate phase; Table S8, percentage of total mercury; Table S9, changes in the percentage of total mercury; Table S10, mean daily load estimates of divalent inorganic mercury, methylmercury, and total mercury; Table S11, estimated mean daily net gains and losses; and Table S12, mean daily load estimates of divalent inorganic mercury, methylmercury, and total mercury (XLSX)

■ AUTHOR INFORMATION

Corresponding Author

Austin K. Baldwin − *U.S. Geological Survey, Boise, Idaho 83702, United States;* orcid.org/0000-0002-6027-3823; Phone: 208-387-1365; Email: akbaldwi@usgs.gov

Authors

Brett A. Poulin − *U.S. Geological Survey, Boulder, Colorado 80303, United States; Department of Environmental Toxicology, University of California Davis, Davis, CA 95616, United States;* orcid.org/0000-0002-5555-7733

Jesse Naymik − *Idaho Power Company, Boise, Idaho 83702, United States*

Charles Hoovestol − *Idaho Power Company, Boise, Idaho 83702, United States*

Gregory M. Clark − *U.S. Geological Survey, Boise, Idaho 83702, United States*

David P. Krabbenhoft − *U.S. Geological Survey, Middleton, Wisconsin 53562, United States;* orcid.org/0000-0003-1964-5020

Complete contact information is available at: https://pubs.acs.org/10.1021/acs.est.9b07103

Notes

The authors declare no competing financial interest.

■ ACKNOWLEDGMENTS

The authors gratefully acknowledge Chris Larsen at Idaho Power Company for assistance in the collection and processing of samples, and Mike Tate, John DeWild, Sarah Janssen, Jake Ogorek, and Christopher Babiarz at the USGS Mercury Research Laboratory for sample analysis. Ralph Myers, Nick

https://dx.doi.org/10.1021/acs.est.9b07103
Environ. Sci. Technol. XXXX, XXX, XXX−XXX

Gastelecutto, Jim Chandler, Sarah Higer, Collin Eagles-Smith, James Willacker, Mark Marvin-DiPasquale, Ron Antweiler, and Reed Harris made valuable contributions to study planning, data interpretation, and discussions. Funding and support were provided by Idaho Power Company, the Idaho Department of Environmental Quality, and the USGS Cooperative Funding, Toxics Substances Hydrology, and Contaminant Biology programs (Environmental Health Mission Area). Any use of trade, product, or firm names is for descriptive purposes only and does not imply endorsement by the U.S. Government.

REFERENCES

(1) Brigham, M. E.; Krabbenhoft, D. P.; Olson, M. L.; DeWild, J. F. Methylmercury in Flood-Control Impoundments and Natural Waters of Northwestern Minnesota, 1997−99. *Water, Air, Soil Pollut.* **2002**, *138* (1−4), 61−78.

(2) Montgomery, S.; Lucotte, M.; Rheault, I. Temporal and Spatial Influences of Flooding on Dissolved Mercury in Boreal Reservoirs. *Sci. Total Environ.* **2000**, *260* (1), 147−157.

(3) Willacker, J. J.; Eagles-Smith, C. A.; Lutz, M. A.; Tate, M. T.; Lepak, J. M.; Ackerman, J. T. Reservoirs and Water Management Influence Fish Mercury Concentrations in the Western United States and Canada. *Sci. Total Environ.* **2016**, *568*, 739−748.

(4) Fleming, E. J.; Mack, E. E.; Green, P. G.; Nelson, D. C. Mercury Methylation from Unexpected Sources: Molybdate-Inhibited Freshwater Sediments and an Iron-Reducing Bacterium. *Appl. Environ. Microbiol.* **2006**, *72* (1), 457−464.

(5) Gilmour, C. C.; Henry, E. A.; Mitchell, R. Sulfate Stimulation of Mercury Methylation in Freshwater Sediments. *Environ. Sci. Technol.* **1992**, *26* (11), 2281−2287.

(6) Gilmour, C. C.; Podar, M.; Bullock, A. L.; Graham, A. M.; Brown, S. D.; Somenahally, A. C.; Johs, A.; Hurt, R. A.; Bailey, K. L.; Elias, D. A. Mercury Methylation by Novel Microorganisms from New Environments. *Environ. Sci. Technol.* **2013**, *47* (20), 11810−11820.

(7) Kerin, E. J.; Gilmour, C. C.; Roden, E.; Suzuki, M. T.; Coates, J. D.; Mason, R. P. Mercury Methylation by Dissimilatory Iron-Reducing Bacteria. *Appl. Environ. Microbiol.* **2006**, *72* (12), 7919−7921.

(8) Canavan, C. M.; Caldwell, C. A.; Bloom, N. S. Discharge of Methylmercury-Enriched Hypolimnetic Water from a Stratified Reservoir. *Sci. Total Environ.* **2000**, *260* (1), 159−170.

(9) Bloom, N. S.; Effler, S. W. Seasonal Variability in the Mercury Speciation of Onondaga Lake (New York). *Water, Air, Soil Pollut.* **1990**, *53* (3), 251−265.

(10) Watras, C. J.; Back, R. C.; Halvorsen, S.; Hudson, R. J.; Morrison, K. A.; Wente, S. P. Bioaccumulation of Mercury in Pelagic Freshwater Food Webs. *Sci. Total Environ.* **1998**, *219* (2−3), 183−208.

(11) Eckley, C. S.; Luxton, T. P.; Goetz, J.; McKernan, J. Water-Level Fluctuations Influence Sediment Porewater Chemistry and Methylmercury Production in a Flood-Control Reservoir. *Environ. Pollut.* **2017**, *222*, 32−41.

(12) McCord, S. A.; Beutel, M. W.; Dent, S. R.; Schladow, S. G. Evaluation of Mercury Cycling and Hypolimnetic Oxygenation in Mercury-Impacted Seasonally Stratified Reservoirs in the Guadalupe River Watershed, California. *Water Resour. Res.* **2016**, *52* (10), 7726−7743.

(13) Kasper, D.; Forsberg, B. R.; Amaral, J. H. F.; Leitão, R. P.; Py-Daniel, S. S.; Bastos, W. R.; Malm, O. Reservoir Stratification Affects Methylmercury Levels in River Water, Plankton, and Fish Downstream from Balbina Hydroelectric Dam, Amazonas, Brazil. *Environ. Sci. Technol.* **2014**, *48* (2), 1032−1040.

(14) Eckley, C. S.; Luxton, T. P.; McKernan, J. L.; Goetz, J.; Goulet, J. Influence of Reservoir Water Level Fluctuations on Sediment Methylmercury Concentrations Downstream of the Historical Black Butte Mercury Mine, OR. *Appl. Geochem.* **2015**, *61*, 284−293.

(15) Zhao, L.; Guo, Y.; Meng, B.; Yao, H.; Feng, X. Effects of Damming on the Distribution and Methylation of Mercury in Wujiang River, Southwest China. *Chemosphere* **2017**, *185*, 780−788.

(16) Bilodeau, F.; Therrien, J.; Schetagne, R. Intensity and Duration of Effects of Impoundment on Mercury Levels in Fishes of Hydroelectric Reservoirs in Northern Québec (Canada). *Inland Waters* **2017**, *7* (4), 493−503.

(17) Slotton, D. G.; Reuter, J. E.; Goldman, C. R. Mercury Uptake Patterns of Biota in a Seasonally Anoxic Northern California Reservoir. *Water, Air, Soil Pollut.* **1995**, *80* (1), 841−850.

(18) Feng, X.; Jiang, H.; Qiu, G.; Yan, H.; Li, G.; Li, Z. Mercury Mass Balance Study in Wujiangdu and Dongfeng Reservoirs, Guizhou, China. *Environ. Pollut.* **2009**, *157* (10), 2594−2603.

(19) Waldron, M. C.; Colman, J. A.; Breault, R. F. Distribution, Hydrologic Transport, and Cycling of Total Mercury and Methyl Mercury in a Contaminated River-Reservoir-Wetland System (Sudbury River, Eastern Massachusetts). *Can. J. Fish. Aquat. Sci.* **2000**, *57* (5), 1080−1091.

(20) Clark, G. M.; Naymik, J.; Krabbenhoft, D. P.; Eagles-Smith, C. A.; Aiken, G. R.; Marvin-DiPasquale, M. C.; Harris, R. C.; Myers, R. Mercury Cycling in the Hells Canyon Complex of the Snake River, Idaho and Oregon; *Fact Sheet; USGS Numbered Series 2016−3051*; U.S. Geological Survey: Reston, VA, 2016; p 6.

(21) Myers, R.; Harrison, J.; Parkinson, S. K.; Hoelscher, B.; Naymik, J.; Parkinson, S. E. *Pollutant Transport and Processing in the Hells Canyon Complex*; Idaho Power Company 2003.

(22) Ebel, W. J.; Koski, C. H. Physical and Chemical Limnology of Brownlee Reservoir, 1962−64. *Fish. Bull.* **1968**, *67* (2), 295−335.

(23) MacCoy, D. E.; Mebane, C. A. Mercury Concentrations in Water and Mercury and Selenium Concentrations in Fish from Brownlee Reservoir and Selected Sites in the Boise and Snake Rivers, Idaho and Oregon, 2013−17; *Open-File Report; USGS Numbered Series 2018−1122*; U.S. Geological Survey: Reston, VA, 2018.

(24) U.S. Geological Survey. National Water Information System data available on the World Wide Web (USGS Water Data for the Nation) http://dx.doi.org/10.5066/F7P55KJN (accessed Oct 20, 2017).

(25) Olson, M. L.; DeWild, J. F. Techniques for the Collection and Species-Specific Analysis of Low Levels of Mercury in Water, Sediment, and Biota; *Water Resources Investigations Report 99−4018B*; U.S. Geological Survey, 1999.

(26) Olund, S. D.; DeWild, J. F.; Olson, M. L.; Tate, M. T. Methods for the Preparation and Analysis of Solids and Suspended Solids for Total Mercury; *Techniques and Methods; USGS Numbered Series 5-A8*; **2004** DOI: 10.3133/tm5A8.

(27) U.S. Environmental Protection Agency. Method 1631, Revision E: Mercury in Water by Oxidation, Purge and Trap, and Cold Vapor Atomic Fluorescence Spectrometry, **2002**.

(28) U.S. Environmental Protection Agency. Method 1630: Methyl Mercury in Water by Distillation, Aqueous Ethylation, Purge and Trap, and Cold Vapor Atomic Fluorescence Spectrometry, **1998**.

(29) DeWild, J. F.; Olsen, M. L.; Olund, S. D. Determination of Methyl Mercury by Aqueous Phase Ethylation, Followed by Gas Chromatographic Separation with Cold Vapor Atomic Fluorescence Detection; *Open-File Report; USGS Numbered Series 2001−445*; U.S. Geological Survey, 2002; p 19.

(30) Wickam, H.; Francois, R.; Henry, L.; Muller, K. *Dplyr: A Grammar of Data Manipulation*; **2017**.

(31) R Core Team. *R: A Language and Environment for Statistical Computing*, Version 3.6.1; R Foundation for Statistical Computing: Vienna, Austria, 2015.

(32) Giraudoux, P. Pgirmess: Data Analysis in Ecology. *R Package*, Version 1.6.3; **2015**.

(33) Feng, X.; Meng, B.; Yan, H.; Fu, X.; Yao, H.; Shang, L. Mercury in Inflow/Outflow Rivers of Reservoirs. In *Biogeochemical Cycle of Mercury in Reservoir Systems in Wujiang River Basin, Southwest China*; Feng, X., Meng, B., Yan, H., Fu, X., Yao, H., Shang, L., Eds.; Springer Singapore: Singapore, 2018; pp 67−94 DOI: 10.1007/978-981-10-6719-8_5.

https://dx.doi.org/10.1021/acs.est.9b07103
Environ. Sci. Technol. XXXX, XXX, XXX−XXX

(34) Lorenz, D.; Runkel, R.; De Cicco, L. Rloadest: River Load Estimation. *R Package*; **2015**.
(35) Runkel, R. L.; Crawford, C. G.; Cohn, T. A. Load Estimator (LOADEST): A FORTRAN Program for Estimating Constituent Loads in Streams and Rivers; *U.S. Geological Survey Techniques and Methods Book 4*, Chapter A5; **2004** DOI: 10.3133/tm4A5.
(36) Scudder, B. C.; Chasar, L. C.; Wentz, D. A.; Bauch, N. J.; Brigham, M. E.; Moran, P. W.; Krabbenhoft, D. P. Mercury in Fish, Bed Sediment, and Water from Streams Across the United States, 1998−2005; *Scientific Investigations Report; USGS Numbered Series 2009−5109*; U.S. Geological Survey, 2009.
(37) Williams, G. A.; Mink, L. L.; Hill, S. R.; Cochran, A.; Farley, R.; Greenfield, K.; Hudson, W. A.; Kiler, K.; Lucky, M.; Ugstad, D. S.; Ugstad, P. O.; Wickham, L. B.; Williams, D. R. *Mercury and Heavy Metal Contamination in the Jordan Creek Drainage near Silver City, Owyhee County, Idaho*; Idaho Transportation Department: Boise, ID, 1974.
(38) Dittman, J. A.; Shanley, J. B.; Driscoll, C. T.; Aiken, G. R.; Chalmers, A. T.; Towse, J. E.; Selvendiran, P. Mercury Dynamics in Relation to Dissolved Organic Carbon Concentration and Quality during High Flow Events in Three Northeastern U.S. Streams. *Water Resour. Res.* **2010**, *46* DOI: 10.1029/2009WR0083.
(39) Heyes, A.; Miller, C.; Mason, R. P. Mercury and Methylmercury in Hudson River Sediment: Impact of Tidal Resuspension on Partitioning and Methylation. *Mar. Chem.* **2004**, *90* (1), 75−89.
(40) Kim, E.-H.; Mason, R. P.; Porter, E. T.; Soulen, H. L. The Effect of Resuspension on the Fate of Total Mercury and Methyl Mercury in a Shallow Estuarine Ecosystem: A Mesocosm Study. *Mar. Chem.* **2004**, *86* (3), 121−137.
(41) Marvin-DiPasquale, M.; Agee, J.; McGowan, C.; Oremland, R. S.; Thomas, M.; Krabbenhoft, D.; Gilmour, C. C. Methyl-Mercury Degradation Pathways: A Comparison among Three Mercury-Impacted Ecosystems. *Environ. Sci. Technol.* **2000**, *34* (23), 4908−4916.
(42) Black, F. J.; Poulin, B. A.; Flegal, A. R. Factors Controlling the Abiotic Photo-Degradation of Monomethylmercury in Surface Waters. *Geochim. Cosmochim. Acta* **2012**, *84*, 492−507.
(43) Suchanek, T. H.; Eagles-Smith, C. A.; Harner, E. J. Is Clear Lake Methylmercury Distribution Decoupled from Bulk Mercury Loading? *Ecol. Appl. Publ. Ecol. Soc. Am.* **2008**, *18* (8), A107−A127.
(44) Willacker, J. J.; Eagles-Smith, C. A.; Kowalski, B. M.; Danehy, R. J.; Jackson, A. K.; Adams, E. M.; Evers, D. C.; Eckley, C. S.; Tate, M. T.; Krabbenhoft, D. P. Timber Harvest Alters Mercury Bioaccumulation and Food Web Structure in Headwater Streams. *Environ. Pollut.* **2019**, *253*, 636−645.
(45) Schetagne, R.; Doyo, J. F.; Fournier, J. J. Export of Mercury Downstream from Reservoirs. *Sci. Total Environ.* **2000**, *260* (1−3), 135−145.
(46) Kasper, D.; Palermo, E. F. A.; Branco, C. W. C.; Malm, O. Evidence of Elevated Mercury Levels in Carnivorous and Omnivorous Fishes Downstream from an Amazon Reservoir. *Hydrobiologia* **2012**, *694* (1), 87−98.

https://dx.doi.org/10.1021/acs.est.9b07103
Environ. Sci. Technol. XXXX, XXX, XXX−XXX